



PH562 Quantum Optics Essay 2022-23

Temporal Solitons in Optical Fibres

Submitted in partial fulfilment for the degree of *MPhys Physics with Advanced Research*

Lewis MacLeod Russell
Registration No.: 201817988

SUPA Department of Physics, University of Strathclyde, Glasgow G4 0NG, United Kingdom
(Dated: 3rd May 2023)

Abstract

The contents of this essay focus on the propagation and dispersion properties of temporal solitons within optical fibres. Where appropriate, connection to PH562 lecture material has been outlined, primarily in discussion of Kerr-nonlinearity and the Nonlinear Schrödinger Equation (NLSE). An overview of optical fibres and solitons is given, with primary focus revolving around their connections to the NLSE. Lastly, some applications and current limitations within these fibre-optics are considered.

Contents

Abstract	i
List of Figures	ii
I. Introduction	1
II. Brief Overview and History of:	2
A. Solitons, and Distinguishing Temporal From Spatial	2
B. Optical Fibres	3
C. Temporal Soliton Propagation in Optical Fibres	5
III. Nonlinear Schrödinger Equation (NLSE)	7
A. Derivation for Hollow-core Fibres	7
B. Derivation for Photonic Crystal Fibres	10
C. Derivation for Polarisation-maintaining Fibres	14
IV. Applications of Temporal Solitons	16
V. Current Challenges within Temporal Soliton Research	17
VI. Conclusion	17
References	20

List of Figures

1	Cross-Sectional Views of a Typical Single and Multi Mode Optical Fibre	4
2	Cross-Sectional Imaging of Various Specialised Optical Fibre Designs	7
3	Measured Properties of an Example HC-PCF around 850 nm Wavelength	11
4	Schematic of a Proposed Chloroform Clad-filled Temperature Invariant PCF.	12
5	Nonlinearity Coefficient Variation in relation to Wavelength and Temperature for a Proposed Chloroform Clad-filled Temperature Invariant PCF.	13
6	Dispersion Variation in relation to Wavelength and Temperature for a Proposed Chloroform Clad-filled Temperature Invariant PCF.	14

I. Introduction

The globally digitalised world we live in today has undoubtedly relied on many technological breakthroughs in our lifetimes and prior, and the transmission and processing of data represents a crucial sub-domain of our wider technological infrastructure. Over the last fifty-years in particular, the properties of temporal solitons in optical fibres have garnered significant interest due to their potential applications in telecommunications, data transmission, and all-optical signal processing [1–9]. Solitons are self-sustaining waveforms that maintain their shape while travelling through a medium, and the intriguing characteristics of these waves have driven researchers to explore their unique properties and potential uses. This essay will provide an in-depth analysis of temporal solitons in optical fibres, exploring their historical development, mathematical descriptions, and applications in various fields.

The general phenomenon of solitons was first observed in water waves by John Scott Russell in 1844 [10]. Only a mere 35 miles from our university campus at Strathclyde, he was investigating efficiency improvements to canal boat designs on the Union Canal when he noticed that upon the boat being brought to a sudden halt, a large, rounded, and well-defined mass of water would form from the bow of the vessel and would propagate until interrupted by the windings of the canal itself. However, it took a further century to formalise an in-depth description of such waves in nonlinear dispersive media, when in the 1960s these solitons were theoretically described by Martin Kruskal and Norman Zabusky through adaptation of the Korteweg–de Vries (KdV) equation for water waves [11–13]. Subsequently, the concept of solitons was extended to the field of optics with the discovery of temporal solitons in optical fibres by Akira Hasegawa and Fumio Tappert in 1973 [14]. They demonstrated that under certain conditions, optical pulses could propagate through fibres without any significant change in their shape, a phenomenon known as soliton transmission.

One of the critical aspects of understanding temporal solitons is their mathematical description, and the Nonlinear Schrödinger Equation (NLSE) serves as the primary tool for describing soliton propagation in optical fibres. As will be explored primarily in Section III, different types of fibres require unique derivations of the NLSE, which dictate the precise details of soliton behaviour within each fibre type. Although a non-exhaustive list of fibre types, we will isolate the NLSE to traditional cladded fibres in Section II C, and speciality hollow-core, photonic crystal, and polarisation-maintaining fibres in Section III.

The applications of temporal solitons span a wide range of fields, and in Section IV we will explore their usage in: all-optical signal regeneration, optical switching, soliton transmission, ultrashort pulse generation, and wavelength conversion. These applications hold the potential to further revolutionise telecommunications and optical computing, opening new frontiers for high-speed data transmission and processing.

Despite the promising aspects of temporal solitons, several challenges remain in the field. This will be outlined in Section V, where we will address current research hurdles and explore how ongoing developments could help overcome these obstacles. By exploring throughout this essay the properties of these temporal solitons within optical fibres, we aim to provide readers with a comprehensive insight into this intriguing phenomenon and its potential impact on future technologies.

II. Brief Overview and History of:

A. Solitons, and Distinguishing Temporal From Spatial

Whilst we shall be isolating our study of optical solitons to the temporal type throughout this essay, we mustn't overlook spatial solitons for clarity and distinguishment. Both share the same fundamental definition, in that they refer to any optical field or wave that remains unchanged throughout propagation. Mathematically, these solitons arise under conditions where both linear and nonlinear effects in the propagation medium are delicately balanced. However, their differences lie in the following:

1. **Spatial Solitons:** are optical beams that propagate without significant diffraction effects in a nonlinear medium, maintaining their shape and intensity profile over distance. They result from a balance between nonlinear self-(de)focusing and linear diffraction effects, representing self-guided optical fields with transverse confinement in the directions orthogonal to propagation [15]. In simpler terms, they propagate without noticeable diffraction. Solitons of the spatial variety represent those covered in Lectures 15-16 of the PH562 course, and historically, the realisation of spatial solitons came marginally later than their temporal counterpart; 1974 [16] and 1973 [14], respectively [17].
2. **Temporal Solitons:** on the other hand, arise through their ability to balance between the dispersive (variation of the group velocity as a function of the wavelength) and nonlinear (variation of the phase velocity as a function of the wave intensity) effects within their propagation medium [17]. Under spatial confinement of the optical field, such phenomenon can arise.

We will confine our essay to the exploration of solitons that satisfy integrable solutions to the NLSE, as elaborated on in Section III. However, it should be noted that materials exist that can produce spatial solitons in which their behaviours dramatically deviate from an exactly integrable NLSE [18, 19]. Such deviation arises from "Kerr Nonlinearity", in which electric field intensity can alter the refractive index of a material [20]; temporal solitons exclusively arise within Kerr-nonlinearity conforming materials [19], whereas spatial solitons are not subject to such confinement [18].

As was explored in Lectures 15-16 of the PH562 course, the Kerr effect is a nonlinear optical phenomenon where the refractive index of a material depends on the intensity of the light passing through it. This effect plays a significant role in the formation and propagation of temporal solitons propagating through optical fibres, in particular. The provided equations within the aforementioned PH562 Lectures Slides describe the behaviour of light in the presence of Kerr-nonlinearity, which can subsequently be applied to the formation of temporal solitons.

In the first set of these equations from the lecture notes (Equation 1), ψ represents the complex envelope of the optical field, with A being the amplitude and φ being the phase. The variables ζ and δ are normalised distance and detuning parameters, respectively, and \hat{Q} denotes the normalised nonlinear coefficient. The first equation line here describes the evolution of the amplitude and phase of the optical field along the propagation distance ζ , with the second equation line showing the relationship between the phase and the amplitude at any distance ζ .

$$\begin{aligned} \psi &= Ae^{i\varphi} \quad , \quad \frac{\partial A}{\partial \zeta} + iA \frac{\partial \varphi}{\partial \zeta} = -i\delta \hat{Q} A^3 \\ A &= A(0) \quad , \quad \varphi = \varphi(0) - \delta \hat{Q} A^2 \zeta \end{aligned} \quad (1)$$

The next set of equations (Equation 2) describes the relationship between the polarisation P and the electric field F in the presence of Kerr-nonlinearity. The parameter χ is the nonlinear

susceptibility, Q is a constant related to the material properties, I_{sat} is the saturation intensity, and δ is again the detuning parameter. The susceptibility χ is approximated by its linear and nonlinear components as shown, respectively.

$$P = \chi F$$

$$\chi = Q \frac{-1 + i\delta}{1 + \delta^2 + |F|^2/I_{\text{sat}}} \approx i \left(\frac{Q\delta}{1 + \delta^2} - \frac{Q\delta}{(1 + \delta^2)^2 I_{\text{sat}}} |F|^2 \right) \quad (2)$$

The final set of equations (Equation 3) provides the expression for the effective refractive index n_{eff} in terms of the linear refractive index n_0 (χ_{LIN}), the nonlinear refractive index n_2 (χ_{NL}), and the electric field F . The effective refractive index is influenced by the Kerr-nonlinearity, which depends on the intensity of the light $|F|^2$. We can summarise this by stating that the expression for n_{eff} is approximated by considering the contributions from both the linear and nonlinear refractive index susceptibilities of the medium.

$$n_{\text{eff}} = \sqrt{1 + \text{Re}(\chi)} = \sqrt{1 + \text{Re}(\chi_{\text{LIN}}) + \text{Re}(\chi_{\text{NL}})} = \sqrt{n_0^2 + \text{Re}(\chi_{\text{NL}})}$$

$$n_{\text{eff}} \approx n_0 \left(1 + \frac{1}{2n_0^2} \text{Re}(\chi_{\text{NL}}) \right) = n_0 + \frac{1}{2n_0} \frac{Q|\delta|}{(1 + \delta^2)^2 I_{\text{sat}}} |F|^2 = n_0 + n_2 |F|^2 \quad (3)$$

These aforementioned equations describe the behaviour of light in the presence of Kerr-nonlinearity, and its effect on the formation and propagation of temporal solitons in optical fibres will become apparent as this essay progresses. The first set of equations relates the amplitude and phase of the optical field to the propagation distance. The second set of equations describes the relationship between the polarisation and the electric field, taking into account the Kerr-nonlinearity. Finally, the third set of equations provides an expression for the effective refractive index, which is influenced by the intensity-dependent Kerr-nonlinearity. The balance between dispersion and nonlinearity in the optical fibre ultimately leads to the formation and stable propagation of temporal solitons.

One final note regarding the nonlinear contributions of these solitons is their possibility to byproduct stimulated Brillouin and Raman scattering (SBS/SRS), which describe the interaction of acoustic-phonon waves and optical waves, respectively [17, 21]. In SBS, the incident light wave interacts with the coherent movements of atoms being offset from their equilibrium lattice positions (acoustic-phonons), leading to the generation of a backscattered wave at a slightly lower frequency. SRS, on the other hand, involves the interaction of the incident light with molecular vibrational modes, resulting in a scattered wave at a higher or lower frequency, known as the Stokes or anti-Stokes wave [21]. SRS plays a crucial role in Raman amplification, which is used to extend the transmission distance in optical communication systems - we will explore the applicational implications of Raman properties further in Section IV.

B. Optical Fibres

Optical fibres are long, thin strands of optically transparent materials, usually made of glass or plastic, and are designed to transmit light over vast distances with minimal loss. They have become the backbone of modern communication systems, enabling high-speed data transmission with low latency and minimal signal attenuation [4, 22]. The concept of optical fibres dates back to the 19th century, but it was not until the 20th century that they became a reality due to significant advances being made within the fields of materials science and optics.

The first practical optical fibre was developed in 1966 by Charles Kao and George Hockham, who proposed that high-purity glass fibres could be used for communication purposes [23]. At this

time of inception however, optical fibres with low signal attenuation and lasers (for optical source) with appropriate emission spectra were not available [17]. Nevertheless, their groundbreaking work on low-loss optical fibres paved the way for a revolution in telecommunications, eventually leading to the rapid growth of optical fibre networks worldwide; something we can all relate to with our household fibre-optic broadband. Today, optical fibres come in various forms, each designed to meet specific application requirements. In general, they can be categorised into two main types: single-mode fibres (SMF) and multi-mode fibres (MMF) [24, 25]. SMFs support only one mode of light propagation, offering higher bandwidth and longer transmission distances. In contrast, MMFs support multiple modes, which can lead to signal dispersion but are typically more affordable and easier to work with. Figure 1 shows the typical construct of these fibres, for reference.

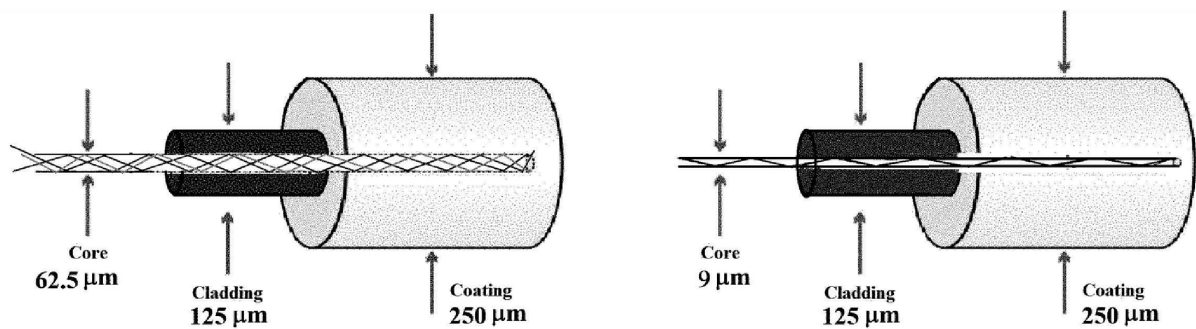


Figure 1: *Cross-Sectional Views of a Typical Single and Multi Mode Optical Fibre*. Left depicts multi-mode fibres (MMF), and right depicts single-mode fibres (SMF). SMFs typically feature a noticeably reduced cross-sectional area of their core in comparison to their MMF counterparts. The core represents the medium in which the light propagates, and the cladding (which must be of a lower refractive index than the core^a in order to allow reflection of the light) serves to maintain this light transmission through the core. The coating simply exists as a protective shielding material to safeguard against physical degradation and exposure to moisture and other external contaminants. Omitted from the figure is a “jacket”, which may also feature in some designs and exist as an additional outer layer containing multiple individual optical fibres within. Figure sourced from Rezgui, 2022 [25].

^a This is technically only true of traditional fibre-optics, however unique exemptions to this rule apply within hollow-core fibres, for example.

The critical properties of optical fibres that make them ideal for temporal soliton generation and propagation are their low loss, low dispersion, and nonlinear characteristics. Low loss is essential to ensure that the soliton maintains its shape over long distances without significant attenuation. This is achieved by using high-purity materials and careful fibre design. Dispersion, referring to the variation of group velocity as a function of wavelength, is a crucial factor in soliton formation. In optical fibres, two primary dispersion mechanisms come into play: chromatic dispersion (caused by the wavelength dependence of the refractive index) and waveguide dispersion (caused by the geometry of the fibres' two main sections, the core and cladding) - the latter is analogous to the windings of the Union Canal disrupting Russell's observation of self-sustaining water waves [10]. For soliton formation, the dispersion must be carefully managed to balance the nonlinear effects that arise from the intensity dependence of the refractive index, typically due to the Kerr effect, as mentioned previously in Section II A.

Nonlinear properties are another vital aspect of optical fibres that contribute to the generation and propagation of temporal solitons. As discussed earlier, the Kerr effect plays a significant role in the formation of temporal solitons, where the refractive index of the material depends on the intensity of the light passing through it. The delicate balance between dispersion and nonlinearity in optical fibres allows for the formation of stable temporal solitons that can propagate without significant change in their shape.

C. Temporal Soliton Propagation in Optical Fibres

We have briefly outlined the conceptual background of solitons and fibre-optics separately in the previous two subsections, however, it is the synergistic amalgamation of these theories and properties that are our primary focus. This Section aims to concisely elucidate the process of temporal soliton generation and their propagation in optical fibres, providing a foundation for understanding the key concepts involved. Specifically, we will primarily focus on SMF descriptions.

Temporal solitons within optical fibres are formed when the dispersive and nonlinear effects in the fibre precisely balance each other out. To better understand this process, we can consider the role of the Kerr effect, as outlined earlier in Section II A. The Kerr effect states that the refractive index of a medium depends on the intensity of the light passing through it. In optical fibres, this intensity-dependent refractive index results in a nonlinear phase shift experienced by the propagating light within the core of the fibre.

On the other hand, dispersion in optical fibres causes different frequency components of the light pulse to propagate at different velocities, leading to pulse broadening [26]. As previously introduced in Section II B, there are two primary dispersion mechanisms in optical fibres: chromatic dispersion and waveguide dispersion. The total dispersion experienced by the light pulse can be expressed as:

$$D_{\text{total}} = D_{\text{chromatic}} + D_{\text{waveguide}} \quad (4)$$

To reiterate, the formation and propagation of temporal solitons in an optical fibre are dictated by the balanced effects of dispersion and nonlinearity contributions. As a mathematical starting point, we can consider linear and nonlinear polarisation terms (right hand side, polarisation represented by \mathbf{P}) in relation to the standard form of Maxwell's electromagnetic wave equation (left hand side, \mathbf{E} representing electric field) in Equation 5 [27]:

$$\nabla^2 \mathbf{E} - \frac{1}{c^2} \frac{\partial^2 \mathbf{E}}{\partial t^2} = \mu_0 \frac{\partial^2 \mathbf{P}_L}{\partial t^2} + \mu_0 \frac{\partial^2 \mathbf{P}_{NL}}{\partial t^2} \quad (5)$$

Since we are considering SMFs only here, we can assume that the electric field is quasi-monochromatic. Furthermore, we can apply the Slowly Varying Amplitude (SVA) Approximation, as explored in Lectures 15-16 of the PH562 course material, outlining the condition that the envelope function $A(z, t)$ varies slowly in time and space compared to the electric field \mathbf{E} itself. In other words, the second-order partial derivatives of \mathbf{E} and \mathbf{P} are negligible in comparison to their first-order counterparts when accounting for angular frequencies ω and wave-numbers k .

First, we take the scalar component of the electric field, $\mathbf{E} = E(z, t) \exp(-i\omega_0 t) \hat{\mathbf{e}}_x$, where ω_0 is the central angular frequency and $\hat{\mathbf{e}}_x$ is the unit vector in the x-direction.

Next, we assume that the linear polarisation term \mathbf{P}_L accounts for material dispersion and fibre loss, while the nonlinear polarisation term \mathbf{P}_{NL} accounts for the nonlinear effects, mainly the Kerr effect, in the fibre.

By substituting the electric field \mathbf{E} into Equation 5 and making the slowly varying amplitude approximation, we can obtain an equation that describes the evolution of the envelope $A(z, t)$. This step involves a few mathematical manipulations, including taking the curl of the equation, applying the chain rule, and eliminating rapidly oscillating terms. The result is a partial differential equation in $A(z, t)$, which given here is the NLSE in the form given in Equation 6; this form of the NLSE captures the interplay between linear dispersion and nonlinear phase shift in a general SMF and can be written as follows:

$$\frac{\partial A(z, t)}{\partial z} + \beta_1 \frac{\partial A(z, t)}{\partial t} + \frac{i\beta_2}{2} \frac{\partial^2 A(z, t)}{\partial t^2} + \frac{\alpha}{2} A = i\gamma(\omega_0) |A(z, t)|^2 A(z, t) \quad (6)$$

The terms in Equation 6 have the following interpretations:

1. $\frac{\partial A}{\partial z}$: The change in the envelope amplitude with respect to the propagation distance, z .
2. $\beta_1 \frac{\partial A}{\partial t}$: The group velocity term, accounting for the delay in the envelope.
3. $\frac{i\beta_2}{2} \frac{\partial^2 A}{\partial t^2}$: The group velocity dispersion (GVD) term, accounting for the spreading of the pulse due to the different group velocities of its frequency components.
4. $\frac{\alpha}{2} A$: The fibre loss term, accounting for attenuation along the fibre.
5. $i\gamma(\omega_0) |A|^2 A$: The nonlinear term, accounting for the Kerr effect, where $\gamma(\omega_0)$ is the nonlinear coefficient, which depends on the central frequency ω_0 .

Thus, Equation 6 is a form of the NLSE derived from Maxwell's electromagnetic wave equation (Equation 5), taking into account the linear and nonlinear polarisation terms, as well as the slowly varying amplitude approximation. The NLSE given here in Equation 6 is very generalised and conforms to the standard description of light propagation in the most common fibre type, known as "cladded fibres"; better tailored versions for specific scenarios will be derived and discussed in greater detail throughout the following section (Section III). For further reading and reference, Equation 6 is adapted from the derivation provided by Agrawal, 2013 [27].

In practice of course, we could negate any of the α or β terms above if a given situation results in a significant difference in the contributions. In other words, if one of these terms happened to be dominant, or one was significantly weaker than the other two, we can disregard their contributions and still arrive at a numerically accurate result. If we were to simplify these terms, the most likely contributions to disregard would be the fibre loss term and the group velocity term, assuming we have a modern high-specification fibre-optic spanning a relatively short travel distance, and that we have a high-quality laser providing little delay to our light envelope. In which case, for example, we could just say that our NLSE cancels these terms out and becomes:

$$\frac{\partial A(z, t)}{\partial z} = -i\frac{\beta_2}{2} \frac{\partial^2 A(z, t)}{\partial t^2} + i\gamma |A(z, t)|^2 A(z, t) \quad (7)$$

where $A(z, t)$ represents the complex electric field envelope, β_2 is the group velocity dispersion (GVD) coefficient, and γ is the nonlinear coefficient. The first term on the right-hand side corresponds to the dispersion (GVD, specifically), while the second term represents the nonlinear phase shift due to the Kerr effect.

To recap, when the dispersion and nonlinearity are balanced within the NLSE, the light pulse evolves into a stable temporal soliton that can propagate over long distances without significant change in its shape or velocity. This balance is achieved when the GVD coefficient and the nonlinear coefficient have specific values that equate to a cancelling of each other's overall effect on wave propagation. The interplay between dispersion and nonlinearity can give rise to different types of solitons, including fundamental solitons and higher-order solitons. Fundamental solitons are the simplest form of solitons, while higher-order solitons have more complex structures, such as pulse splitting and recombination during propagation [28, 29].

Temporal soliton propagation in optical fibres offers numerous benefits in communication systems, such as increased data transmission capacity, reduced signal distortion, and enhanced resilience against perturbations. These advantages stem from the self-preserving nature of solitons, which allows them to maintain their shape and energy over vast distances. This, ultimately, has led to the development of soliton-based communication systems and novel applications in areas such as those to be highlighted in Section IV.

III. Nonlinear Schrödinger Equation (NLSE)

We have already introduced the purpose and generalised form of the NLSE previously in Section II C, and in this Section, we will further explore its usefulness when uniquely adapted for speciality fibre types; the variations of the NLSE presented in this Section should be taken as a small flavour of examples only, and not concretely versatile master equations as every fibre design requires unique consideration. Connection to recent literature will also provide insight into the operating parameters and specifications of these state of the art fibre designs, leading to the discussion of their appropriate use-cases within Section IV. Whilst we have categorised these unique fibre types here into hollow-core, photonic crystal, and polarisation-maintaining, it is not uncommon for advanced designs to merge these into hybridised forms; for example, with hollow-core photonic crystal fibres (HC-PCFs) [30, 31], or polarisation-maintaining photonic crystal fibres [24]. In Figure 2 below, we can visualise the design of some of these advanced fibre-optics via cross-sectional electron-microscopy.

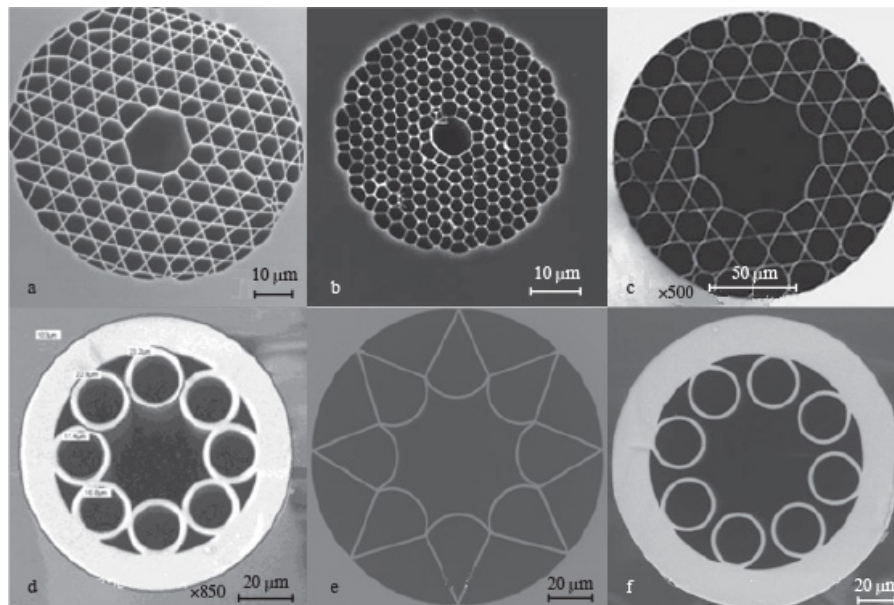


Figure 2: *Cross-Sectional Electron-Microscopy Imaging of Various Specialised Optical Fibre Designs.* **a, b, c**, showcase various HC-PCFs; **d, e, f**, showcase various revolver-type HC fibres.
Figure sourced from Gladyshev, 2015 [32].

A. Derivation for Hollow-core Fibres

Hollow-core fibres (HCFs) are a unique type of optical fibre designed with a central air-filled or gas-filled core, surrounded by a cladding structure [6, 30–32]. This design differs from traditional solid-core fibres, which typically consist of a solid glass or silica core; as a result, the hollow-core unintuitive features a lower reflective index in comparison to the cladding, and therefore the transmitted light can no longer rely on total-internal-reflection to guide propagation direction. Instead, other guiding mechanisms must be utilised which typically rely on HCF cladding being formed by either a microstructured arrangement of air holes [6, 32] or a photonic bandgap structure [30, 31].

The key advantage of hollow-core fibres is that they exhibit extremely low material absorption and nonlinearity since the light propagates mainly through the air or gas in the core rather than through the solid material. This results in lower signal attenuation and reduced dispersion, enabling longer transmission distances and higher data rates. In addition, HCFs exhibit lower latency compared to solid-core fibres since light travels faster in air or gas than in solid materials. This characteristic is

particularly useful for applications requiring real-time communication and data transfer.

Gas-filled HCFs also offer unique possibilities for gas sensing, as the gas-filled core allows for direct interaction between the guided light and the target gas molecules, enhancing the sensitivity of the sensor [4, 24].

However, there are some challenges associated with hollow-core fibres, such as increased sensitivity to bending losses and potential difficulties in coupling light efficiently into and out of the fibre. Despite these challenges, the numerous advantages offered by HCFs have led to significant research and development efforts in recent years, resulting in continuous improvements in their performance and expanding their potential applications.

For example, one such recent paper (Safaei, 2020) achieved enhanced multi-dimensional solitary state (MDSS) generation within large-core, nitrogen-filled, HCFs [33]. The researchers demonstrate the creation of MDSS (including both temporal and spatial soliton generation) using multimillijoule, subpicosecond near-infrared pulses and investigate the underlying physics, determining that the spatial and temporal localisation of MDSS enables the compression of broadened pulses to 10.8 fs by simple linear propagation in fused silica. Prior to their publication, they note that considerable work on conventional one-dimensional HCFs waveguides already existed, however their aim was to create a novel demonstration of effective MDSS generation with strong spatiotemporal coherence and power scalability within their HCF design.

We can refer to their provided Supplementary Material for a summary of their NLSE considerations [33]. The one-dimensional simulations presented within their paper are modelled via the NLSE as [33, 34]:

$$\frac{\partial A}{\partial z} + \frac{1}{2} \left(\alpha(\omega_0) + i\alpha_1 \frac{\partial}{\partial t} \right) A - i \sum_{n=1}^{\infty} i^n \frac{\beta_n}{n!} \frac{\partial^n A}{\partial t^n} = i \left(\gamma(\omega_0) + i\gamma_1 \frac{\partial}{\partial t} \right) \left(A(z, t) \int_0^{\infty} R(t') |A(z, t - t')|^2 dt' \right) \quad (8)$$

Due to the many terms involved within Equation 8, it is useful if we list a description of each term as follows:

1. A : The complex amplitude of the optical field.
2. z : The propagation distance along the fibre.
3. t : Time variable.
4. ω_0 : The reference frequency of the optical field.
5. $\alpha(\omega_0)$: The linear attenuation at the reference frequency ω_0 .
6. α_1 : The first-order derivative of the attenuation with respect to frequency.
7. β_n : The n th-order dispersion coefficient, which characterises the dispersion properties of the fibre.
8. $\gamma(\omega_0)$: The nonlinear coefficient at the reference frequency ω_0 , which is related to the fibre's nonlinear response.
9. γ_1 : The first-order derivative of the nonlinear coefficient with respect to frequency.
10. $R(t')$: The Raman response function, which describes the time dependence of the Raman gain in the fibre.
11. t' : Dummy variable used in the integral over the Raman response function.

The left-hand side of the equation represents the evolution of the optical field A along the propagation distance z , considering linear effects such as attenuation and dispersion. The right-hand side represents the nonlinear contribution to the field evolution, including the Raman effect and the self-phase modulation due to the intensity-dependent refractive index. Whilst we have discussed intensity-dependent refractive indexes via the Kerr-nonlinearity within the PH562 classes, the details of the Raman effect and self-phase modulation are beyond the primary scope of this essay. However, it is necessary to state their existence as they do play a vital role in the dynamics of soliton propagation. In summary, the Raman effect (as mentioned in Section II A) is a nonlinear optical phenomenon in which incident light interacts with molecular vibrations in a medium, resulting in frequency-shifted scattered light. Self-phase modulation is another nonlinear optical effect where a light pulse modifies its own phase due to these intensity-dependent refractive index changes in the medium.

However, the NLSE must further be adapted when applied in the context of high-power applications where there is a necessity to describe the multimode aspects associated to large-mode cross-sectional fibre core areas. This is then known as the “Generalised Multimode NLSE” (GMMNLSE), and Safaei et al [33] describe the dynamics of their modal envelope via Equation 9 as:

$$\begin{aligned} \frac{\partial A_p(z, t)}{\partial z} = & i \left(\beta_0^p - R[\beta_0^0] \right) A_p - i \left(\beta_1^p - R[\beta_1^0] \right) \frac{\partial A_p(z, t)}{\partial t} + i \sum_{n=2}^{\infty} i^n \frac{\beta_n^p}{n!} \frac{\partial^n A_p}{\partial t^n} + \\ & i \frac{n_2 \omega_0}{c} \left(1 + \frac{i}{\omega_0} \frac{\partial}{\partial t} \right) \sum_{l, m, n} \left[(1 - f_R) S_{plmn}^k A_l A_m A_n^* + \right. \\ & \left. f_R A_l S_{plmn}^R \int_0^{\infty} h_R(t) A_m(z, t - t') A_n^*(z, t - t') dt' \right] \end{aligned} \quad (9)$$

Furthermore, they specify that they are launching linearly polarised light into their fibres, in which case, S_{plmn}^k and S_{plmn}^R can be defined as per Equation 10 [3]:

$$S_{plmn}^k = S_{plmn}^R = \frac{\int dxdy F_P F_l F_m F_n}{\left[\int F_P^2 dxdy \int F_l^2 dxdy \int F_m^2 \int F_n^2 \right]^{1/2}} \quad (10)$$

Equation 9 describes the evolution of the complex modal amplitudes¹ $A_p(z, t)$ along the fibre as a function of distance z and time t . It is a further adaptation of the Nonlinear Schrödinger Equation (NLSE) for multimode fibers, incorporating both linear (dispersion) and nonlinear (Kerr and Raman) effects. Collectively, the terms in this equation account for the modal dispersion coefficients, the nonlinear refractive index, the central angular frequency, the fractional Raman response, and the overlap integrals for nonlinear interactions; and, more specifically, each term describes the following:

1. $A_p(z, t)$: The complex modal amplitude of the p -th mode as a function of distance z and time t .
2. $\beta_0^p, \beta_1^p, \beta_n^p$: The n -th order dispersion coefficients for the p -th mode.
3. $R[\beta_0^0], R[\beta_1^0]$: The reference dispersion coefficients for the fundamental mode.

¹ As an interesting and supplementary side note, a comprehensive understanding of harmonics and modal frequencies can be gathered through the study of musical acoustics [35]. The description of harmonics within electromagnetic waves and the NLSE is often unintuitive and feature complex mathematical models; in contrast, the harmonic behaviours observed in acoustic waves are easier to describe and can serve as an appropriate and analogous reference point for understanding frequency harmonics and modes.

4. n_2 : The nonlinear refractive index of the medium.
5. ω_0 : The central angular frequency of the input pulse.
6. c : The speed of light in a vacuum.
7. f_R : The fractional contribution of the delayed Raman response.
8. S_{plmn}^k, S_{plmn}^R : The overlap integrals for the Kerr and Raman nonlinear interactions, respectively.
9. $h_R(t)$: The Raman response function.
10. F_p, F_l, F_m, F_n : The transverse mode profiles of the interacting modes p, l, m, n .

Equation 10 defines the overlap integrals S_{plmn}^k and S_{plmn}^R for the Kerr and Raman nonlinear interactions, respectively. These integrals represent the degree of spatial overlap between the interacting modes p, l, m, n , and are crucial for describing the strength of nonlinear interactions in multimode fibres. The equation calculates the integrals by considering the transverse mode profiles F_p, F_l, F_m, F_n and integrating over the transverse x and y directions orthogonal to the z direction of propagation [3].

In summary of their paper, Equation 9 primarily governed the dynamics of MDSSs and allowed Safaei et al [33] to successfully generate high-energy and stable multimode beams through appropriately balanced linear and nonlinear contributions.

B. Derivation for Photonic Crystal Fibres

Photonic Crystal Fibres (PCFs) are a special class of optical fibres that employ a periodic arrangement of microstructures in the cladding region designed to guide and manipulate light [2, 24, 30, 31, 36–38]. These fibres consist of a core region surrounded by a cladding, which contains a periodic array of air holes or dielectric inclusions that run along the entire length of the fibre. The unique structure of PCFs gives rise to novel optical properties and capabilities not achievable with traditional optical fibres.

Unlike conventional fibres, which rely on total-internal-reflection (TIR) to confine light within the core, PCFs can guide light using two different mechanisms: modified total internal reflection and photonic bandgap guidance. In the first case, the periodic structure of the cladding modifies the effective refractive index of the cladding, while in the second case, the cladding structure forms a photonic bandgap that prevents certain wavelengths of light from propagating in the cladding, thus confining them within the core. PCFs offer several advantages and unique features compared to conventional fibres.

Better control over signal distortion is possible via highly customisable and tailored dispersion profiles [2], translating into stable soliton generation and propagation and better control over signal distortion. Their small core sizes and tight confinement of light leads to significantly higher nonlinearity than conventional fibres also - convenient for applications within all-optical signal processing and wavelength conversion (See Section IV). PCFs can also perform single-mode operation over a large range of wavelengths, particularly beneficial for applications requiring high spectral purity or low signal distortion; in some designs, they can even be purposely limited to “endlessly single-mode” operation for deployment in applications where high signal fidelity and low modal dispersion is prioritised. In such operation, propagation only supports a single spatial mode, regardless of the wavelength of the beam [36, 37]. In more recent years, the hybridisation of PCFs with HCFs has also been investigated to harness the combined advantages from both concepts - such designs create significantly reduced nonlinearity, low latency, and the ability to guide light in unconventional

wavelength regions. Figure 3 provides additional clarity on the confinement of propagated light in such fibres, and the low dispersion profile in this example is evident.

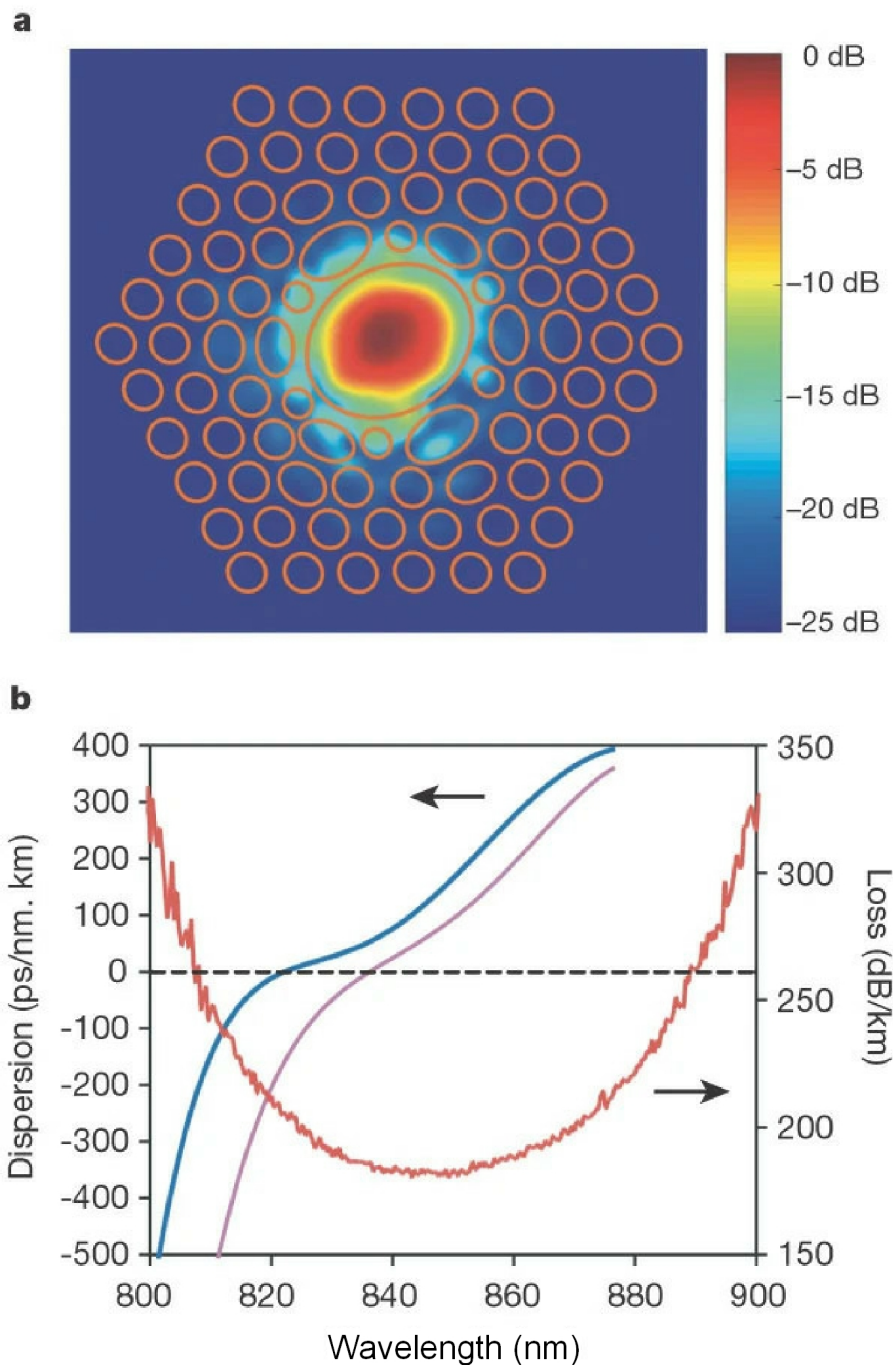


Figure 3: *Measured Properties of an Example HC-PCF around 850 nm Wavelength.* **a**, A logarithmic graph illustrating the near-field pattern at 848nm wavelength after travelling a distance of 60 meters through the fibre. The initial few rings of air holes are depicted schematically in terms of their positions and shapes, and the heatmap highlights the core's ability to strongly confines the light, with only a minuscule fraction overlapping with silica. **b**, The fibre's observed loss and dispersion characteristics are shown. The minimum loss is 180 dB/km at an 850 nm wavelength, likely limited by leakage. Dispersion remains low and anomalous throughout much of the guiding band, facilitating soliton propagation. The two lines featuring inflection points around zero-dispersion represent the two fundamental polarisation modes in this design; these are split due to structural deformation. Figure sourced from Knight, 2003 [2].

Let's now return our focus again to solid-core PCFs. The temperature of a PCF can sufficiently alter the width of its spectral output, even within the range of typical room temperatures. This is an undesirable effect in applications which dictate a reliance on temperature independent spectral output and soliton-based communications, and hence a recent model was proposed for a temperature independent chloroform clad-filled PCF design [38]. In this study, Dhasarathan et al employed the NLSE to analyse the spectral output of their fibre design and the nonlinearity and dispersion properties across a range of temperature and fibre parameters. Their proposed design featured negligible spectral width variance (0.1nm/C) across typical room temperature values (20C - 40C), and a cross-sectional schematic of this proposed fibre is shown below in Figure 4.

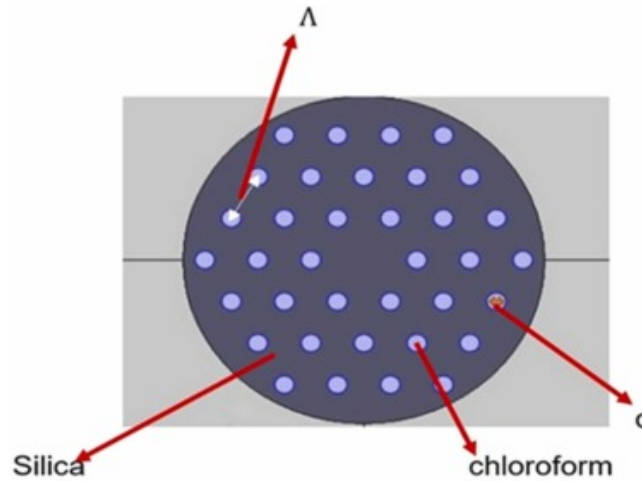


Figure 4: *Schematic of a Proposed Chloroform Clad-filled Temperature Invariant PCF.* The geometric parameters labelled are: Λ , for pitch, set to $2.2\mu m$ centre-to-centre separation; d , simply the hole diameter, varied from $1\mu m$ to $0.4\mu m$. A negative rate of refractive index variation with temperature is associated to the capillaries filled with chloroform, whereas the silica in contrast features a positive such differential. Figure sourced from Dhasarathan, 2022 [38].

Their range of capillary cladding diameters were specified as $d=1, 0.8, 0.48$ and $0.4 \mu m$, and the nonlinear coefficients γ within their NLSE were calculated through Equation 11 as:

$$\gamma = \frac{2\pi n_2}{\lambda A_{eff}} \quad (11)$$

n_2 and λ have their usual meaning, representing the nonlinear refractive index and wavelength, respectively; A_{eff} represents the effective area of the fundamental mode. In general, the properties of PCFs are substantially affected by their geometric construct (See Figure 4), and hence dispersion profiles will differ between different fibre construct parameters. Dispersion, $D(\lambda, T)$, can be calculated via a second-order differential equation shown below in Equation 12. T , representing temperature, contributes to the value of the overall effective refractive index n_{eff} , the exact values of which can be obtained from the original literature [38].

$$D(\lambda, T) = \frac{-\lambda}{c} \frac{d^2 n_{eff}}{d\lambda^2} \quad (12)$$

Their form of the NLSE is not too dissimilar to what we have seen in Equation 8 within Section III A. In fact, by simply adapting the notation given by Dhasarathan et al and rearranging within Equation 13, we arrive back at an approximation of Equation 8:

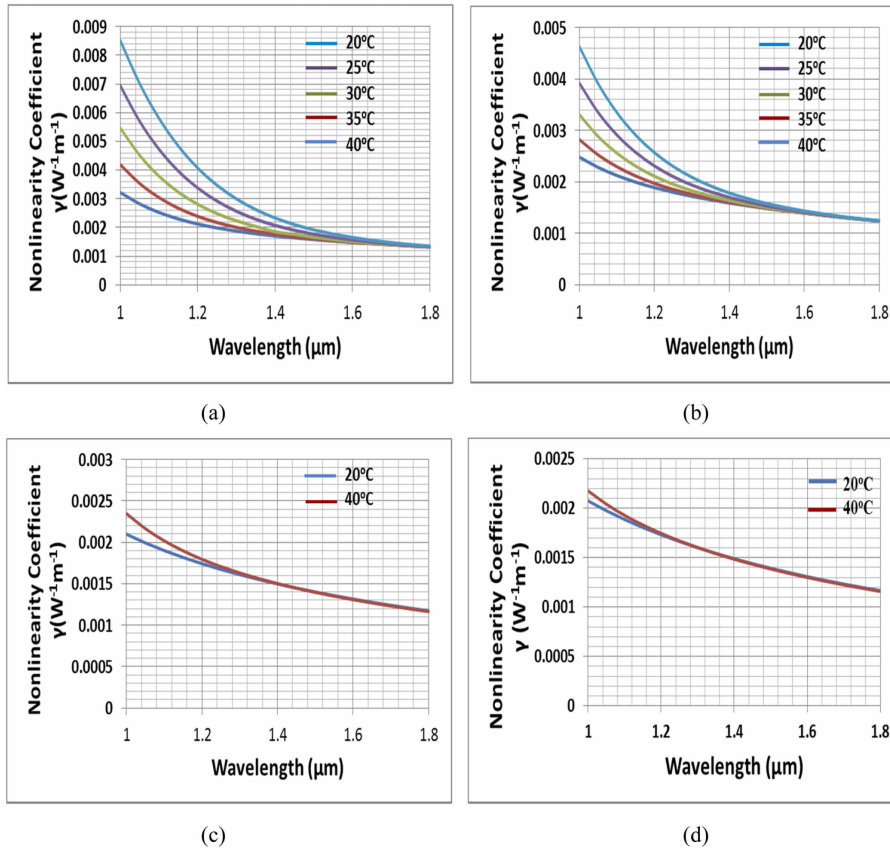


Figure 5: *Nonlinearity Coefficient Variation in relation to Wavelength and Temperature for a Proposed Chloroform Clad-filled Temperature Invariant PCF.* Capillary cladding diameters are associated to each of the four plots as: **a)**, $1\mu m$, **b)**, $0.8\mu m$, **c)**, $0.48\mu m$, **d)**, $0.4\mu m$. Figure sourced from Dhasarathan, 2022 [38].

$$\begin{aligned}
 \frac{\partial U}{\partial z} + \sum_{n=2}^4 \beta_n \frac{i^{n-1}}{n!} \frac{\partial^n U}{\partial t^n} + \frac{\alpha}{2} U &= i\gamma \left(1 + i\tau_{\text{shock}} \frac{\partial}{\partial t} \right) \times \left(U(z, t) \int_{-\infty}^{\infty} R(t') |U(z, t - t')|^2 dt' \right) \\
 \frac{\partial A}{\partial z} + \sum_{n=2}^4 \beta_n \frac{i^{n-1}}{n!} \frac{\partial^n A}{\partial t^n} + \frac{\alpha}{2} A &= i\gamma \left(1 + i\tau_{\text{shock}} \frac{\partial}{\partial t} \right) \left(A(z, t) \int_{-\infty}^{\infty} R(t') |A(z, t - t')|^2 dt' \right) \\
 \frac{\partial A}{\partial z} + \frac{\alpha(\omega_0)}{2} + \sum_{n=2}^4 \beta_n \frac{i^{n-1}}{n!} \frac{\partial^n A}{\partial t^n} &= i \left(\gamma(\omega_0) + i\gamma_1 \frac{\partial}{\partial t} \right) \left(A(z, t) \int_{-\infty}^{\infty} R(t') |A(z, t - t')|^2 dt' \right) \\
 \therefore \frac{\partial A}{\partial z} + \frac{\alpha(\omega_0)}{2} - i \sum_{n=2}^4 i^n \frac{\beta_n}{n!} \frac{\partial^n A}{\partial t^n} &= \\
 i \left(\gamma(\omega_0) + i\gamma_1 \frac{\partial}{\partial t} \right) \left(A(z, t) \int_{-\infty}^{\infty} R(t') |A(z, t - t')|^2 dt' \right) & \quad (13)
 \end{aligned}$$

We can hence conclude that Dhasarathan et al have utilised a simplified form of the NLSE which excludes the first-order derivative of the attenuation with respect to frequency; furthermore, only the n -order dispersion coefficients are considered for $n = \{2, 3, 4\}$. It is unclear from the literature why the fundamental (first-order) dispersion coefficient is omitted, although context surrounding the generation of solitons is still provided via Equation 14 in the form of:

$$N = T_p \sqrt{\frac{\gamma P}{\beta_2}} \quad (14)$$

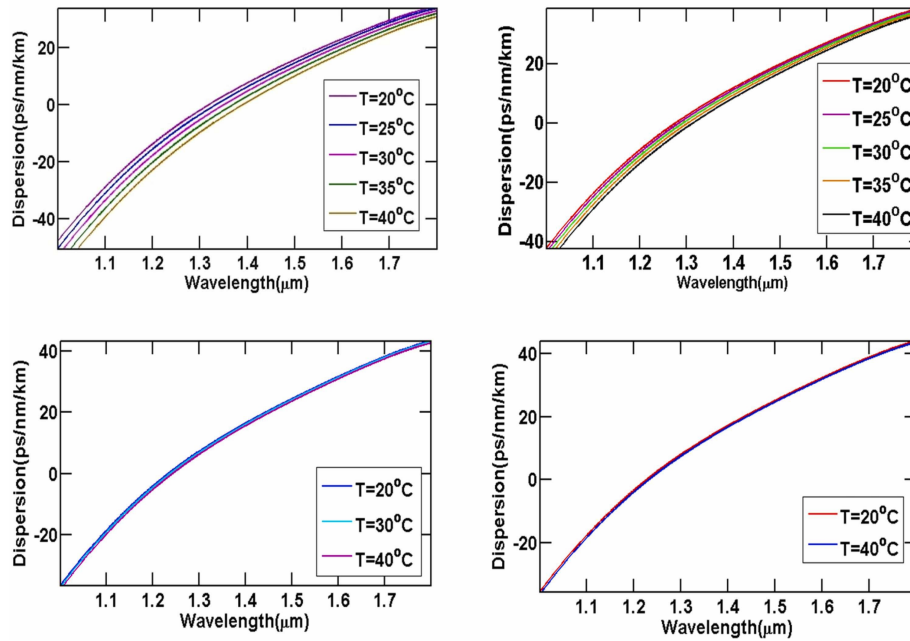


Figure 6: Dispersion Variation in relation to Wavelength and Temperature for a Proposed Chloroform Clad-filled Temperature Invariant PCF. Capillary cladding diameters are associated to each of the four plots as: **a)**, $1\mu m$, **b)**, $0.8\mu m$, **c)**, $0.48\mu m$, **d)**, $0.4\mu m$. Figure sourced from Dhasarathan, 2022 [38].

This introduces a dependency on some newly introduced terms T_p and P , input pulsewidth and pulse peak power, respectively. N is an integer-squared value representing an n th-order soliton; $N = 1$ dictates the generation of a fundamental soliton in which original pulse formation is maintained across large propagation distances, and values greater than one represent higher-order solitons in which the temporal shape is instead oscillatory and periodic [34, 39]. Inclusive of γ and β_2 , a full table of the nonlinear coefficient values used can be found numerically defined in the literature [38].

To conclude our overview of their paper, two figures are provided (Figures 5 and 6) which highlight that a reduction to the core diameters' results in an overall reduction in the temperature sensitivity associated to both nonlinear contributions and dispersion.

C. Derivation for Polarisation-maintaining Fibres

Optical fibres of the polarisation-maintaining (PM) variety are specialised in maintaining the polarisation state of propagating light [3, 7, 24, 27, 34, 39–44]. Their popularity within fibre design research originally dates back to the mid-1980s [40, 41, 44], and nowadays these PM fibres are attracting attention for quantum information applications that rely on the polarisation of entangled photons being communicated [42]. In standard single-mode fibres, the polarisation state of the light can change over time and distance due to external factors such as stress, temperature changes, and imperfections in the fibre. This variation can cause signal degradation and impair system performance in certain applications, such as coherent optical communications or Quantum Key Distribution set-ups [45–48]; maintaining a consistent polarisation state is crucial in such applications.

To preserve the polarisation state, PM fibres employ a unique design that introduces a strong birefringence between two orthogonal polarisation modes within the fibre; the term “birefringence” refers to the optical property of materials which will change their refractive index depending on the polarisation or propagation direction of light. This birefringence creates a significant difference in the propagation constants for the two polarisation modes, thus minimising the coupling between them

and maintaining the input polarisation state throughout the length of the fibre. PM fibre designs are essential for applications which mandate the preservation of polarisation states for optimal performance.

There are two primary types of PM fibres: PANDA fibres [40], and bow-tie fibres [44]. PANDA fibres have a circular core surrounded by two stress-inducing regions made of a different glass type and with a higher thermal expansion coefficient. The stress regions are typically in the shape of an ellipse or resemble the shape of panda eyes, hence the name PANDA fibres. Bow-tie fibres, which again take their name from their distinctive shape, feature stress-inducing bow-tie shaped regions and are placed on opposite sides of the core. This geometric design creates birefringence, which helps maintain the polarisation state of the propagating light.

Most PM fibres are linearly birefringent, meaning that they have two primary axes that facilitate undisturbed polarisation of linearly polarised light [7]. Recalling the method described for obtaining the NLSE in Section II C, we can adapt the generalised NLSE shown previously in Equation 5 to represent linear birefringence in Equation 16.

Firstly, the electric field can be factored out into transverse dependences of E_j (Equation 15), where $j = x, y$. $F(x, y)$ defines the spatial distribution of the fundamental mode supported by the fibre, $A_j(z, t)$ is assumed to be a slowly varying amplitude, and β_{0j} represents a propagation constant.

$$\mathbf{E}_j(\mathbf{r}, t) = F(x, y)A_j(z, t) \exp(i\beta_{0j}z) \quad (15)$$

The dispersive effects are included by expanding the frequency-dependent propagation constant β_{0j} in a similar manner to methods described in the literature [27]. The slowly varying amplitudes, A_x and A_y , are found to satisfy the following set of two coupled-mode NLSE equations [7]:

$$\begin{aligned} \frac{\partial A_x}{\partial z} + \beta_{1x} \frac{\partial A_x}{\partial t} + \frac{i\beta_2}{2} \frac{\partial^2 A_x}{\partial t^2} + \frac{\alpha}{2} A_x = \\ i\gamma \left(|A_x|^2 + \frac{2}{3} |A_y|^2 \right) A_x + \frac{i\gamma}{3} A_x^* A_y^2 \exp(-2i\Delta\beta z) , \\ \frac{\partial A_y}{\partial z} + \beta_{1y} \frac{\partial A_y}{\partial t} + \frac{i\beta_2}{2} \frac{\partial^2 A_y}{\partial t^2} + \frac{\alpha}{2} A_y = \\ i\gamma \left(|A_y|^2 + \frac{2}{3} |A_x|^2 \right) A_y + \frac{i\gamma}{3} A_y^* A_x^2 \exp(2i\Delta\beta z) . \end{aligned} \quad (16)$$

where,

$$\Delta\beta = \beta_{0x} - \beta_{0y} = (2\pi/\lambda)B_m = 2\pi/L_B \quad (17)$$

is correlated to the fibre's linear birefringence. The two polarisations both share and do not share some common parameters. For example, the first-order chromatic dispersion coefficients β_{1x} and β_{1y} are in general not equal to one another, since the two polarisation components are governed by separate group velocities. Contrasty, parameters evaluated at the same wavelength λ will be equal for both polarisation components (nonlinear coefficients β_2 and γ).

This linear birefringence is only one example, and considerations for elliptically birefringent fibres [7] or circular and linear polarisation in multimode designs [33] can be found within the cited literature [7, 33].

As a side note regarding connection to PH562 material, we have seen how to solve coupled differential equations similar in style to Equation 16 within the "Collective Effects in Light-Matter Interactions" Lectures. Albeit, these lectures started from the toy-model example on damped harmonic oscillators and then covered damping effects and spontaneous emission for two-level atoms. Although conceptually unrelated to our coupled-NLSE for linearly birefringent PM fibres, similarities in their mathematical modelling are shared.

IV. Applications of Temporal Solitons

Within this Section, we outline a non-exhaustive list of some potential applications which exploit the properties of temporal solitons within optical fibres. We can also consider the properties of some of the fibre types outlined in Section III, and propose which applications may be best suited to a given fibre design. Specifically, we briefly cover: all-optical signal regeneration, optical switching, soliton transmission, ultrashort pulse generation, and wavelength conversion.

Beginning with all-optical signal regeneration, this is a promising application suitable for both standard fibre-optics and photonic crystal fibres. In standard fibre-optics, the balance of dispersion and nonlinearity can be adjusted to achieve stable soliton propagation and signal regeneration. Photonic crystal fibres, however, are designed to have a high degree of nonlinearity, which is useful in achieving stable soliton propagation. All-optical signal regeneration using photonic crystal fibres has been demonstrated to overcome dispersion-induced pulse broadening and is particularly useful for long-distance optical communication [1–3].

Optical switching using temporal solitons in optical fibres is another promising application that can benefit from hollow-core fibres. Hollow-core fibres have a unique structure that allows for lower dispersion and reduced nonlinear effects. This makes them particularly well-suited for high-speed optical switching systems [4, 5], where fast response times and low-loss are crucial. In contrast, traditional fibres have high dispersion, making them less suitable for the fast switching speeds required in these systems.

Soliton transmission is an important application of temporal solitons in optical fibres and can be achieved using both standard fibre-optics and photonic crystal fibres. Standard fibre-optics are widely used in optical communication systems and can support soliton propagation over larger distances. In contrast, photonic crystal fibres, which have a high degree of nonlinearity, are useful for soliton transmission over shorter distances or for applications where size and power consumption are important factors [2, 3].

Ultrashort pulse generation is another application that takes advantage of the nonlinear properties of temporal solitons, and it is ideally suited for polarisation-maintaining fibres [8] or even hollow-core fibres [6]. Polarisation-maintaining fibres are designed to maintain the polarisation direction of light propagating through them. This leads to stable pulsed laser operation with improved output power, stability and beam quality. They are particularly well-suited for laser applications, where precision and stability are required [7–9, 45, 46].

Our last application under consideration is that of wavelength conversion, of which photonic crystal fibres tend to be well-suited here due to their high nonlinearity, which allows for efficient wavelength conversion [2, 8, 9, 49]. In photonic crystal fibres, the high degree of nonlinearity depends on the specific fibre design, and this can be tailored to achieve the desired wavelength conversion effect. Wavelength conversion is useful in the creation of multi-wavelength optical networks with different wavelengths used to transmit different types of information. Therefore, photonic crystal fibres are useful in many applications, including optical communication, sensing and spectroscopy.

To broadly summarise: standard fibre-optics are widely used and most commonly found within general optical communication systems; photonic crystal fibres (PCFs) and hollow-core fibres (HCFs) are ideal for applications that require high nonlinearity or low dispersion, respectively (See Section III); hybridisation of these PCFs and HCFs (HC-PCFs) produced a strong molecular response via Raman Scattering and are widely used within gas sensing applications as a result [4, 5, 24]; polarisation-maintaining fibres are well-suited for certain laser applications and quantum systems [8, 45–48]; and photonic crystal fibres are generally most suited for wavelength conversion applications [8, 9, 49]. Most importantly, it is vital to choose the best suited fibre-optic for a given application; each have their own selling points and drawbacks, and so the optimal fibre-design is very much dependent on the most critical and necessary properties required.

V. Current Challenges within Temporal Soliton Research

With regards to optical fibres, most of the current limitations lie within practical engineering restraints rather than unfulfilled scientific anomalies. One of the main challenges in the study of temporal solitons is their stability and reproducibility. Even small changes in fibre parameters or environmental conditions can affect the properties of solitons. Researchers are working to develop new methods to stabilise and control solitons, such as through the use of microresonators [50–53].

Of course, the same nonlinear effects that enable the formation of solitons can also lead to undesired effects for given applications such as spectral broadening and distortion [26]. Dispersion-managed fibres [54] form only a fraction of this wider field of research. Furthermore, there is not a single point for improvement, and advancements will vary from one use-case to another: in all-optical signal regeneration, for example, one challenge faced is the ability to regenerate signals in the presence of noise [1]; in soliton transmission, challenges fundamentally concern the ability to maintain soliton stability over long distances [55].

And perhaps the most dominant limitation above all else is cost. An improved fibre-optic design for enhanced soliton generation and propagation will only gain wider-spread adoption and accessibility if it is cost-effective and commercially viable. PCFs are a prime example, requiring complex and precise manufacturing techniques that make them expensive, cost-prohibitive, and low-production yield items [2]. Perhaps this is why photonic bandgap HCFs or HC-PCFs have garnered interest, given their ability to achieve similar nonlinear effects with simpler manufacturing methods [30, 31, 55, 56].

VI. Conclusion

We have seen throughout this essay that the phenomenon of temporal solitons propagating through optical fibres has captured the attention of researchers and engineers alike. Despite our modern digitalised infrastructure relying on such principles, their research into advanced design prevails in the interest of increased data transmission and communication demands. From their initial observation in water waves by John Scott Russell to the discovery of temporal solitons in optical fibres by Akira Hasegawa and Fumio Tappert, the understanding of solitons has evolved significantly.

The mathematical description of temporal solitons, as detailed by the Nonlinear Schrödinger Equation (NLSE), has provided a powerful tool for understanding soliton propagation in various types of optical fibres and is still relevant even a century past from its first inception. The adaptation of the NLSE for traditional cladded fibres, hollow-core fibres, photonic crystal fibres, and polarisation-maintaining fibres has allowed researchers to gain further insight into soliton behaviour within each fibre type.

The wide range of fibre-optic applications capable of harnessing temporal soliton phenomenon highlights the versatile nature of this physical characteristic. As these applications continue to be developed and refined, they hold the potential to significantly impact telecommunications and optical computing, paving the way for the next generation of high-speed data transmission and processing, classical or quantum.

However, it is important to acknowledge the challenges and limitations that persist in the field of temporal solitons. Addressing these hurdles through ongoing research and development will be essential to fully harness the potential of solitons in optical fibres.

Ultimately, the study of temporal solitons in optical fibres provides a valuable understanding through which to examine the advancement of modern technology. As researchers continue to examine the unique properties and applications of solitons, the future of telecommunications and data transmission can be further transformed by these self-sustaining waveforms.

References

- [1] John M Dudley and J Roy Taylor. Ten years of nonlinear optics in photonic crystal fibre. *Nature Photonics*, 3(2):85–90, 2009.
- [2] Jonathan C Knight. Photonic crystal fibres. *nature*, 424(6950):847–851, 2003.
- [3] Peter Horak and Francesco Poletti. Multimode nonlinear fibre optics: theory and applications. *Recent progress in optical fiber research*, 3, 2012.
- [4] Byoungcho Lee. Review of the present status of optical fiber sensors. *Optical fiber technology*, 9(2):57–79, 2003.
- [5] Yonas Muanenda, Claudio J Oton, and Fabrizio Di Pasquale. Application of raman and brillouin scattering phenomena in distributed optical fiber sensing. *Frontiers in Physics*, 7:155, 2019.
- [6] Andrey D. Pryamikov, Alexander S. Biriukov, Alexey F. Kosolapov, Victor G. Plotnichenko, Sergei L. Semjonov, and Evgeny M. Dianov. Demonstration of a waveguide regime for a silica hollow - core microstructured optical fiber with a negative curvature of the core boundary in the spectral region $> 3.5 \mu\text{m}$. *Opt. Express*, 19(2):1441–1448, 2011.
- [7] Govind P. Agrawal. Chapter 6 - polarization effects. In Govind P. Agrawal, editor, *Nonlinear Fiber Optics (Sixth Edition)*, pages 189–244. Academic Press, sixth edition edition, 2019.
- [8] Fetah Benabid, G Bouwmans, JC Knight, P St J Russell, and F Couny. Ultrahigh efficiency laser wavelength conversion in a gas-filled hollow core photonic crystal fiber by pure stimulated rotational raman scattering in molecular hydrogen. *Physical review letters*, 93(12):123903, 2004.
- [9] Thomas V Andersen, Karen Marie Hilligsøe, Carsten K Nielsen, Jan Thøgersen, KP Hansen, Søren R Keiding, and Jakob J Larsen. Continuous-wave wavelength conversion in a photonic crystal fiber with two zero-dispersion wavelengths. *Optics Express*, 12(17):4113–4122, 2004.
- [10] J.S Russell. Report on waves. *Report of the fourteenth meeting of the British Association for the Advancement of Science*, pages 311–390, 1845.
- [11] N. J. Zabusky and M. D. Kruskal. Interaction of solitons in a collisionless plasma and the recurrence of initial states. *Phys. Rev. Lett.*, 15:240–243, 1965.
- [12] Clifford S Gardner, John M Greene, Martin D Kruskal, and Robert M Miura. Method for solving the korteweg-devries equation. *Physical review letters*, 19(19):1095, 1967.
- [13] Martin D Kruskal, Robert M Miura, Clifford S Gardner, and Norman J Zabusky. Korteweg-devries equation and generalizations. v. uniqueness and nonexistence of polynomial conservation laws. *Journal of Mathematical Physics*, 11(3):952–960, 1970.
- [14] Akira Hasegawa and Frederick Tappert. Transmission of stationary nonlinear optical pulses in dispersive dielectric fibers. i. anomalous dispersion. *Applied Physics Letters*, 23(3):142–144, 1973.
- [15] Yuri S. Kivshar, Govind P. Agrawal, and Govind P. Agrawal. Chapter 1 - introduction. In Yuri S. Kivshar, Govind P. Agrawal, and Govind P. Agrawal, editors, *Optical Solitons*, pages 1–30. Academic Press, Burlington, 2003.
- [16] JE Bjorkholm and AA Ashkin. Cw self-focusing and self-trapping of light in sodium vapor. *Physical Review Letters*, 32(4):129, 1974.
- [17] AKIRA Hasegawa. Optical solitons in fibers: theoretical review. *Optical Solitons—Theory and Experiment*, Cambridge Univ. Press, Cambridge, pages 1–29, 1992.
- [18] Yuri S. Kivshar, Govind P. Agrawal, and Govind P. Agrawal. Chapter 2 - spatial solitons. In Yuri S. Kivshar, Govind P. Agrawal, and Govind P. Agrawal, editors, *Optical Solitons*, pages 31–62. Academic Press, Burlington, 2003.
- [19] Yuri S. Kivshar, Govind P. Agrawal, and Govind P. Agrawal. Chapter 3 - temporal solitons. In Yuri S. Kivshar, Govind P. Agrawal, and Govind P. Agrawal, editors, *Optical Solitons*, pages 63–103. Academic Press, Burlington, 2003.
- [20] P Weinberger. John kerr and his effects found in 1877 and 1878. *Philosophical Magazine Letters*, 88(12):897–907, 2008.

- [21] Y. R. Shen and N. Bloembergen. Theory of stimulated brillouin and raman scattering. *Phys. Rev.*, 137:A1787–A1805, 1965.
- [22] Jim Jachetta. Fiber-optic transmission systems. *National Association of Broadcasters Engineering Handbook*, 2007.
- [23] K Charles Kao and George A Hockham. Dielectric-fibre surface waveguides for optical frequencies. *IET*, 113(7):1151–1158, 1966.
- [24] Bo Dong, Da-Peng Zhou, and Li Wei. Temperature insensitive all-fiber compact polarization-maintaining photonic crystal fiber based interferometer and its applications in fiber sensors. *J. Light-wave Technol.*, 28(7):1011–1015, 2010.
- [25] Hayat Rezgui. An overview of optical fibers. *Global Journal of Science Frontier Research*, 21:14–20, 2022.
- [26] Govind Agrawal. Chapter 3 - group-velocity dispersion. In Govind Agrawal, editor, *Nonlinear Fiber Optics (Fifth Edition)*, Optics and Photonics, pages 57–85. Academic Press, Boston, fifth edition edition, 2013.
- [27] Govind Agrawal. Chapter 2 - pulse propagation in fibers. In Govind Agrawal, editor, *Nonlinear Fiber Optics (Fifth Edition)*, Optics and Photonics, pages 27–56. Academic Press, Boston, fifth edition edition, 2013.
- [28] Jinendra K Ranka, Robert W Schirmer, and Alexander L Gaeta. Observation of pulse splitting in nonlinear dispersive media. *Physical Review Letters*, 77(18):3783, 1996.
- [29] C Daraio, D Ngo, VF Nesterenko, and F Fraternali. Highly nonlinear pulse splitting and recombination in a two-dimensional granular network. *Physical Review E*, 82(3):036603, 2010.
- [30] Francesco Poletti, Marco N Petrovich, and David J Richardson. Hollow-core photonic bandgap fibers: technology and applications. *Nanophotonics*, 2(5-6):315–340, 2013.
- [31] Seyedmohammad Abokhamis Mousavi, Hans Christian Hansen Mulvad, Natalie V Wheeler, Peter Horak, John Hayes, Yong Chen, Thomas D Bradley, Shaif-ul Alam, Seyed Reza Sandoghchi, Eric Numkam Fokoua, et al. Nonlinear dynamic of picosecond pulse propagation in atmospheric air-filled hollow core fibers. *Optics express*, 26(7):8866–8882, 2018.
- [32] A.V. Gladyshev, A.N. Kolyadin, A.F. Kosolapov, Yu.P. Yatsenko, A.D. Pryamikov, A.S. Biriukov, I.A. Bufetov, and E.M. Dianov. Efficient raman generation in a hydrogen-filled hollow-core fibre. *Quantum Electronics*, 45(9):807, 2015.
- [33] Reza Safaei, Guangyu Fan, Ojoon Kwon, Katherine Légaré, Philippe Lassonde, Bruno E Schmidt, Heide Ibrahim, and François Légaré. High-energy multidimensional solitary states in hollow-core fibres. *Nature Photonics*, 14(12):733–739, 2020.
- [34] Govind P Agrawal. Nonlinear fiber optics. In *Nonlinear Science at the Dawn of the 21st Century*, pages 195–211. Springer, 2000.
- [35] Arthur H Benade. *Fundamentals of musical acoustics*. Courier Corporation, 1990.
- [36] Niels Asger Mortensen, Jacob Riis Folken, Peter MW Skovgaard, and Jes Broeng. Numerical aperture of single-mode photonic crystal fibers. *IEEE Photonics Technology Letters*, 14(8):1094–1096, 2002.
- [37] Kunimasa Saitoh and Masanori Koshiba. Single-polarization single-mode photonic crystal fibers. *IEEE Photonics Technology Letters*, 15(10):1384–1386, 2003.
- [38] Vigneswaran Dhasarathan, A. Sharafali, Thien Khanh Tran, EP Mubashira Banu, and M.S. Mani Rajan. Temperature independent photonic crystal fiber for spectroscopic and soliton pulse applications. *Optik*, 271:170155, 2022.
- [39] Akira Hasegawa. *Optical solitons in fibers*. Springer Science & Business Media, 2013.
- [40] Y Sasaki, K Tajima, and S Seikai. 26 km-long polarisation-maintaining optical fibre. *Electronics Letters*, 23(3):127–128, 1987.
- [41] Jan Dorosz and Ryszard Romaniuk. Exotic optical fibres. *SPIE*, 1085:273–276, 1990.
- [42] Guilherme B Xavier and Gustavo Lima. Quantum information processing with space-division multiplexing optical fibres. *Communications Physics*, 3(1):9, 2020.

- [43] EA Zlobina, Sergey Ivanovich Kablukov, and Sergei A Babin. Continuous-wave parametric oscillation in polarisation-maintaining optical fibre. *Quantum Electronics*, 41(9):794, 2011.
- [44] Chen Yijiang and Huang Hung-Chia. Analytical solution of bow-tie fibres. *Electronics Letters*, 22(13):713–715, 1986.
- [45] Nicolas Gisin and Rob Thew. Quantum communication. *Nature photonics*, 1(3):165–171, 2007.
- [46] Stefano Pirandola, Jens Eisert, Christian Weedbrook, Akira Furusawa, and Samuel L Braunstein. Advances in quantum teleportation. *Nature photonics*, 9(10):641–652, 2015.
- [47] Stefano Pirandola and Samuel L Braunstein. Physics: Unite to build a quantum internet. *Nature*, 532(7598):169–171, 2016.
- [48] Stephanie Wehner, David Elkouss, and Ronald Hanson. Quantum internet: A vision for the road ahead. *Science*, 362(6412):eaam9288, 2018.
- [49] Amir Herzog, Avishay Shamir, and Amiel A Ishaaya. Wavelength conversion of nanosecond pulses to the mid-ir in photonic crystal fibers. *Optics letters*, 37(1):82–84, 2012.
- [50] AB Matsko, AA Savchenkov, and L Maleki. On excitation of breather solitons in an optical microresonator. *Optics letters*, 37(23):4856–4858, 2012.
- [51] Wei Liang, Anatoliy A Savchenkov, Vladimir S Ilchenko, Danny Eliyahu, David Seidel, Andrey B Matsko, and Lute Maleki. Generation of a coherent near-infrared kerr frequency comb in a monolithic microresonator with normal gvd. *Optics letters*, 39(10):2920–2923, 2014.
- [52] Myoung-Gyun Suh, Qi-Fan Yang, Ki Youl Yang, Xu Yi, and Kerry J Vahala. Microresonator soliton dual-comb spectroscopy. *Science*, 354(6312):600–603, 2016.
- [53] Philipp Trocha, Maxim Karpov, Denis Ganin, Martin HP Pfeiffer, Arne Kordts, S Wolf, J Krockenberger, Pablo Marin-Palomo, Claudius Weimann, Sebastian Randel, et al. Ultrafast optical ranging using microresonator soliton frequency combs. *Science*, 359(6378):887–891, 2018.
- [54] Thomas F Carruthers, Irl N Duling, Moshe Horowitz, and Curtis R Menyuk. Dispersion management in a harmonically mode-locked fiber soliton laser. *Optics letters*, 25(3):153–155, 2000.
- [55] Govind P Agrawal. *Applications of nonlinear fiber optics*. Elsevier, 2001.
- [56] RF Cregan, BJ Mangan, JC Knight, TA Birks, P St J Russell, PJ Roberts, and DC Allan. Single-mode photonic band gap guidance of light in air. *science*, 285(5433):1537–1539, 1999.